Chemical Engineering Communications

ISSN: 0098-6445 (Print) 1563-5201 (Online) Journal homepage: www.tandfonline.com/journals/gcec20

SYNERGISTIC EFFECT OF N,N-BIS(PHOSPHONOMETHYL) GLYCINE AND ZINC IONS IN CORROSION CONTROL OF CARBON STEEL IN COOLING WATER SYSTEMS

B. V. Appa Rao, M. Venkateswara Rao, S. Srinivasa Rao & B. Sreedhar

To cite this article: B. V. Appa Rao, M. Venkateswara Rao, S. Srinivasa Rao & B. Sreedhar (2011) SYNERGISTIC EFFECT OF N,N-BIS(PHOSPHONOMETHYL) GLYCINE AND ZINC IONS IN CORROSION CONTROL OF CARBON STEEL IN COOLING WATER SYSTEMS, Chemical Engineering Communications, 198:12, 1505-1529, DOI: 10.1080/00986445.2010.525200

To link to this article: https://doi.org/10.1080/00986445.2010.525200

Published online: 22 Aug 2011.

Chem. Eng. Comm., 198:1505–1529, 2011

ISSN: 0098-6445 print/1563-5201 online
DOI: 10.1080/00986445.2010.525200

Taylor & Francis
Taylor & Francis Group

Synergistic Effect of N,N-Bis(phosphonomethyl) Glycine and Zinc Ions in Corrosion Control of Carbon Steel in Cooling Water Systems

B. V. APPA RAO,[1] M. VENKATESWARA RAO,[1]
S. SRINIVASA RAO,[1] AND B. SREEDHAR[2]

[1]Department of Chemistry, National Institute of Technology Warangal (NITW), Warangal, Andhra Pradesh, India
[2]Inorganic and Physical Chemistry Division, Indian Institute of Chemical Technology, Hyderabad, Andhra Pradesh, India

A protective film has been developed on the surface of carbon steel in low chloride aqueous environment using a synergistic mixture of an environmentally friendly phosphonic acid, N,N-bis(phosphonomethyl) glycine (BPMG), and zinc ions. Impedance studies of the metal/solution interface indicated that the surface film is highly protective against the corrosion of carbon steel in the chosen environment. Potentiodynamic polarization studies showed that the inhibitor is a mixed inhibitor. X-ray photoelectron spectroscopic analysis (XPS) of the film showed the presence of the elements iron, phosphorus, nitrogen, oxygen, carbon, and zinc. Deconvolution spectra of these elements in the surface film showed the presence of oxides/hydroxides of iron(III), $Zn(OH)_2$, and [Zn(II)-BPMG] complex. This inference is further supported by the reflection absorption Fourier transform infrared spectrum of the surface film. Analysis by SEM is presented for both the corroded and protected metal surfaces. Based on all these results, a plausible mechanism of corrosion inhibition is proposed.

Keywords BPMG; Carbon steel; Impedance; Inhibitor film; Synergism; XPS

Introduction

Carbon steel is the primary material used in the fabrication of cooling water systems and other industrial water distribution systems. In order to control corrosion of carbon steel in such systems, application of corrosion inhibitors is a widely used method. Due to environmental restrictions imposed on heavy metal ion based corrosion inhibitors, the focus has been shifted to environmentally friendly corrosion inhibitors (Choi et al., 2002). Phosphonates, which were originally introduced as scale inhibitors in water treatment, were later proved to also be good corrosion inhibitors (Awad and Turgoose, 2004). Their impact on the environment was reported to be negligible at the concentration levels used for corrosion inhibition (Jaworska et al., 2002; Awad, 2005a). The use of phosphonic acids for the protection of carbon steel

Address correspondence to B. V. Appa Rao, Department of Chemistry, National Institute of Technology Warangal (NITW), Warangal-506004, Andhra Pradesh, India. E-mail: boyapativapparao@rediffmail.com; chemysri@yahoo.com

from corrosion has been the subject of work reported by several researchers (Choi et al., 2002; Gonzalez et al., 1996; Rajendran et al., 1999a,b; Awad, 2005b; Amar et al., 2003; Felhosi et al., 1999; Reznik et al., 2008; Demadis et al., 2005a; Shaban et al., 1993; Pech-Canul and Chi-Canul, 1999; Paszternak et al., 2007, 2010; Pech-Canul and Bartolo-Perez, 2004; Telegdi et al., 2001). Among the phosphonic acids, 1-hydroxyethane-1,1-diphosphonic acid (HEDP) and aminotris (methylenephosphonic acid) (AMP) are extensively studied and widely used as corrosion inhibitors. They show synergistic effect with zinc ions and form complexes (Choi et al., 2002; Gonzalez et al., 1996; Rajendran et al., 1999a, b; Awad, 2005b; Felhosi et al., 1999; Reznik et al., 2008; Demadis et al., 2005a). A phosphonated amino acid, N-phosphonomethyl glycine, containing one phosphonic acid group, was also reported to be an effective corrosion inhibitor for carbon steel (Shaban et al., 1993; Pech-Canul and Chi-Canul, 1999; Pech-Canul and Bartolo-Perez, 2004).

A phosphonated glycine, N,N-bis(phosphonomethyl) glycine (BPMG), containing two phosphonic acid groups has been chosen in the present study. It is an environmentally friendly phosphonic acid (Telegdi et al., 2001). Apart from the two phosphonic acid groups, it consists of one carboxylic acid group and one amino group. BPMG is also known to form complexes with metal ions like Fe^{2+}, Fe^{3+}, and Zn^{2+} (Sawada et al., 2000; Westerback et al., 1965). No studies on this compound as corrosion inhibitor for carbon steel in aqueous chloride environment have been reported so far in the literature. The objectives of the present study are to investigate the inhibitive properties of the surface film formed by the binary inhibitor system BPMG-Zn^{2+} on carbon steel in the presence of chloride and nearly neutral aqueous environment and to discuss the mechanistic aspects of corrosion inhibition. For all these studies, 200 ppm of sodium chloride solution was chosen as the control because of the following reason: the water used in cooling water systems is generally either demineralized water or unpolluted surface water. In either case, the aggressiveness of the water does not normally exceed that of 200 ppm of NaCl solution.

Experimental Procedures

Materials

For all the studies, the specimens taken from a single sheet of carbon steel of the following composition were chosen: C: 0.1–0.2%, P: 0.03–0.08%, S: 0.02–0.03%, Mn: 0.4–0.5%, and the rest iron. Prior to the tests, the specimens were polished with 1/0, 2/0, 3/0, and 4/0 grade emery polishing papers respectively, further polished to mirror finish with alumina powder on a polishing cloth fixed to a rotating disc, washed with distilled water, degreased with acetone, and dried. For gravimetric measurements, the polished specimens of the dimensions 3.5 cm × 1.5 cm × 0.2 cm were used, while for electrochemical and surface analytical studies, the dimensions of the specimens were 1.0 cm × 1.0 cm × 0.1 cm. Electrochemical studies were carried out at an optimum immersion period of 1 h, and for the surface analytical studies, the immersion period was seven days. N,N-bis(phosphonomethyl) glycine (BPMG), obtained from Aldrich Chemical Company Inc., USA, was used as such in the present study. The molecular structure of BPMG is shown in Figure 1. Zinc sulfate ($ZnSO_4$. $7H_2O$), sodium chloride, and other reagents were analytical grade chemicals. All the solutions were prepared using triple-distilled non-deaerated water, and pH values of the solutions were adjusted using 0.01 N NaOH and 0.01 N

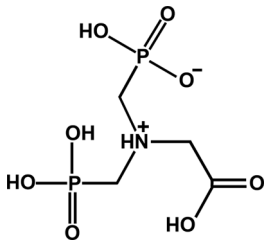

Figure 1. Molecular structure of BPMG.

H_2SO_4 solutions. An aqueous solution consisting of 200 ppm of sodium chloride was used as the control throughout the studies.

Gravimetric Measurements

A modified protocol was used based on NACE Standard TM0169-95 (Item no. 21200; National Association of Corrosion Engineers, Houston). Carbon steel specimens were prepared according to this well-established protocol. Each specimen, after its polishing to mirror finish, was immersed in the control solution in the absence or presence of various inhibitor formulations at pH = 7.0. Corrosion progress was monitored by visual inspection for seven days. Then the specimens were removed from the solution and corrosion products were cleaned by the standard NACE method mentioned above to determine corrosion rates from weight loss.

For all the gravimetric experiments, the polished specimens were immersed in duplicate in 100 mL control solution in the absence and presence of inhibitor formulations of different concentrations. During the studies, only those results were taken into consideration in which the difference in the weight loss of the two specimens immersed in the same solution did not exceed 0.1 mg. Accuracy in weighing up to 0.01 mg and in surface area measured up to 0.1 cm^2, as recommended by ASTM G31, was followed (ASTM Standard G 31-72, 2004). The immersion period of seven days was fixed in view of the considerable magnitude of the corrosion rate obtained in the absence of any inhibitor after this immersion period. The immersion period was maintained accurately up to 0.1 h in view of the lengthy immersion period of 168 h. Under these conditions of accuracy, the relative standard error in corrosion rate determination is of the order of 2% or less for an immersion time of 168 h (Freeman and Silverman, 1992). Inhibition efficiency values (IE_g) of the inhibitor formulations were calculated using the formula

$$IE_g\ (\%) = 100\left[(CR)_O - (CR)_I\right]/(CR)_O \tag{1}$$

where $(CR)_O$ and $(CR)_I$ are the corrosion rates in the absence and presence of inhibitor respectively.

The gravimetric studies were carried out to determine the inhibition efficiencies of BPMG alone, Zn^{2+} alone, and mixtures of BPMG and Zn^{2+} at different concentrations of each. The effect of pH on inhibition efficiency was determined in the case of a few binary inhibitor formulations that showed an inhibition efficiency >90% at pH 7.

Electrochemical Studies

Both the electrochemical impedance spectroscopic (EIS) studies and potentiodynamic polarization studies were carried out using Electrochemical Workstation Model IM6e (Zahner-electrik, GmbH, Germany), and the experimental data were analyzed using Thales software. The measurements were conducted in a conventional three-electrode cylindrical glass cell with platinum electrode as auxiliary electrode and saturated calomel electrode (SCE) as reference electrode. The working electrode was carbon steel embedded in epoxy resin of polytetrafluoroethylene so that a flat surface of $1\,cm^2$ was the only surface exposed to the electrolyte. The three-electrode setup was immersed in 500 mL control solution both in the absence and presence of various inhibitor formulations and allowed to attain a stable open circuit potential (OCP). The pH values of the solutions were adjusted to 7.0 and the solutions were unstirred during the measurements.

Impedance spectra in the form of Nyquist plots were recorded at OCP in the frequency range from 60 kHz to 10 mHz with 4 to 10 steps per decade. A sine wave with 10 mV amplitude was used to perturb the system. The impedance parameters, charge transfer resistance (R_{ct}), constant phase element (CPE), and CPE exponent (n), were obtained from Nyquist plots. The inhibition efficiency values (IE_i) were calculated using the equation

$$IE_i\ (\%) = 100[1 - (R_{ct}/R'_{ct})] \tag{2}$$

where R_{ct} and R'_{ct} are the charge transfer resistance values in the absence and presence of the inhibitor respectively.

Polarization curves were recorded in the potential range of -650 to -150 mV with a resolution of 2 mV. The curves were recorded in the dynamic scan mode with a scan rate of 2 mV/s. The ohmic drop compensation was made during the studies. The corrosion potential (E_{corr}), corrosion current density (I_{corr}), and anodic Tafel slope (β_a) and cathodic Tafel slope (β_c) were obtained by extrapolation of anodic and cathodic regions of the Tafel plots. The inhibition efficiency values (IE_p) were calculated from I_{corr} values using the equation (Elachouri et al., 1996)

$$IE_p\ (\%) = 100[1 - (i'_{corr}/i_{corr})] \tag{3}$$

where i_{corr} and i'_{corr} are the corrosion current densities in the case of the control and inhibitor solutions respectively.

Surface Analysis by X-ray Photoelectron Spectroscopy (XPS)

XPS measurements of the surface films were carried out with a Kratos analytical photoelectron spectrometer model AXIS 165 with monochromated Al K_α X-ray source (1486.6 eV) operated at 100 W and with a resolution of 0.1 eV. Both the survey spectra and deconvolution spectra were recorded at four spots on each specimen. The average of the four measurements is reported. The spectra were collected at an electron take-off angle of 90°. Analyzer pass energy was 80 eV, with a step of 0.1 eV for the elements of interest, namely Fe 2p, P 2p, N 1s, C 1s, O 1s, and Zn 2p. Binding energies for the deconvolution spectra were corrected individually for each measurement set, based on a value of 285.0 eV for the C–C component of C 1s.

Fourier Transform-Infrared (FT-IR) Spectroscopic Studies

FT-IR spectra were recorded using an FT-IR spectrophotometer from Thermo Electron Corporation (USA), model Nexus 670, with a resolving power of $0.125\,cm^{-1}$. The detector is temperature stabilized deuterated triglycine sulfate (DTGS) (KBr window) and liquid nitrogen cooled mercury cadmium tellurium (MCT-A) and the beam splitter is an XT-KBr. FT-IR spectrum of pure BPMG was recorded using the KBr pellet method. The reflection absorption FT-IR spectra of the surface films were recorded in the wave number range of $4000–400\,cm^{-1}$. The measurements were made at a grazing angle of 85°.

Surface Analysis by Scanning Electron Microscopy (SEM)

SEM images were recorded using an FEI Quanta FEG 200 High Resolution Scanning Electron Microscope for the specimens immersed in the control as well as in the inhibitor solution at two different magnifications.

Results and Discussion

Gravimetric Studies

The results of gravimetric studies using the binary system BPMG-Zn^{2+} at various concentrations of both constituents are shown in Figure 2. It is evident that BPMG alone and Zn^{2+} alone accelerate corrosion of carbon steel. BPMG at higher concentrations ($\geq$80 ppm) shows an inhibition efficiency (IE) less than 3%, which is negligible. If the formulations containing both BPMG and Zn^{2+} are considered, combinations with BPMG $\leq$ 20 ppm and Zn^{2+} (20−100 ppm) accelerate the corrosion, and a few show an inhibition efficiency less than 9%. Excellent protection with IE > 90% is achieved with a synergistic mixture of BPMG and Zn^{2+} at the required minimum concentrations of 40 ppm and 30 ppm respectively. In terms of molar concentrations, the required minimum concentrations of BPMG and Zn^{2+}

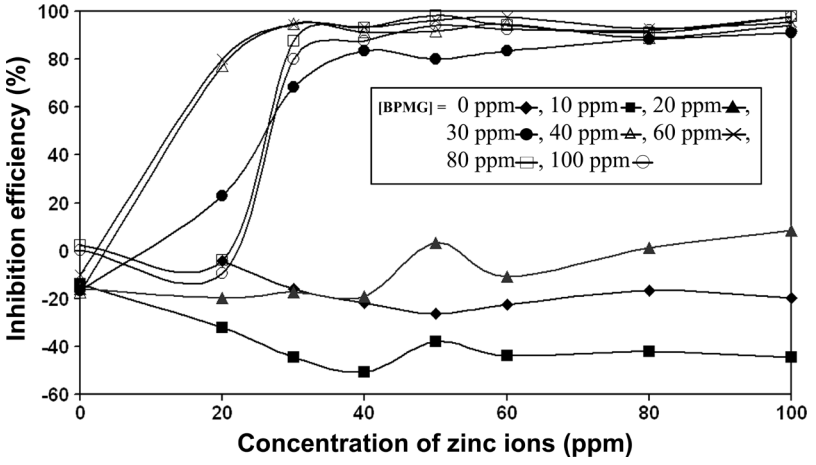

Figure 2. Corrosion inhibition efficiency of the binary system BPMG-Zn^{2+} at pH 7, as a function of concentration of Zn^{2+}.

are 1.5×10^{-4} M and 4.6×10^{-4} M, respectively, the molar ratio of [BPMG]/[Zn^{2+}] being nearly 1:3. At a given concentration of Zn^{2+} of 30 ppm, when the concentration of BPMG in the mixture is greater than 60 ppm, the IE is decreased. However, at higher concentrations of Zn^{2+} (50–100 ppm), the IE is least affected by the increase in concentration of BPMG within the range studied. These results indicate that optimum concentrations of both BPMG and Zn^{2+} are required to obtain strong synergism. Various compositions of the binary inhibitor system showing IE > 90% at pH 7 are shown in Table I.

Good inhibition efficiency values are obtained at 1:2 molar ratio of BPMG/Zn^{2+} and also at other molar ratios up to 1:10 for BPMG/Zn^{2+}. These calculations indicate the significance of the presence of zinc ions in enhancing IE due to synergism. Telegdi et al. (2001) reported potentiostatic polarization studies on the synergistic effect of bivalent ions Ba^{2+}, Sr^{2+}, and Zn^{2+} in the presence of BPMG to inhibit corrosion of Armco iron in 0.1 M $NaClO_4$ solution. They reported that the highest IE values are obtained in the case of all the three cations in the synergistic mixtures of BPMG/cation at the molar ratio of 1:2 with BPMG at a concentration of 3×10^{-4} M. They also mentioned that a relatively thick surface layer was formed on an iron specimen in the presence of BPMG and Zn^{2+} when compared with the combinations containing other cations. It is worth mentioning the molar ratios corresponding to the highest IE values in the case of other phosphonate-Zn^{2+} combinations reported in the literature. For HEDP-Zn(II) system, at the molar ratio of [HEDP]/[Zn^{2+}] of 1:3 and at the concentration of 3×10^{-4} M HEDP, the highest IE was reported (Felhosi et al., 1999). In the case of AMP, at the molar ratio of [AMP]/[Zn^{2+}] of 1:1, the highest IE was obtained at comparable concentrations (Kalman et al., 1993). Complexation constants ($\log K_s$) of HEDP and AMP with Zn^{2+}, each of them at the concentration of 2×10^{-3} M, in aqueous 0.1 M KNO_3 solution, were reported in the literature (Deluchat et al., 1997); the highest value of $\log K_s$ was for the complex between Zn(II) and completely deprotonated ligand. The authors also reported an increase in complexed cation level with an increase in pH from 5 to 8 and a decrease at pH 9. This trend is more evident in the case of HEDP, with the $\log K_s$ value of 10.3, which is much less than the $\log K_s$ value of 16.3 for AMP. This trend

Table I. Various formulations of the binary inhibitor system showing inhibition efficiency >90% at pH = 7.0

[BPMG] (ppm)	[Zn^{2+}] (ppm)	BPMG/Zn^{2+} Molar ratio	I.E. (%)	[BPMG] (ppm)	[Zn^{2+}] (ppm)	BPMG/Zn^{2+} Molar ratio	I.E. (%)
40	30	1:3.0	95	60	100	1:7.0	95
40	40	1:4.0	91	80	40	1:2.0	93
40	50	1:5.0	91	80	50	1:2.5	98
40	60	1:6.0	94	80	60	1:3.0	94
40	100	1:1.0	94	80	80	1:4.0	90
60	30	1:2.0	94	80	100	1:5.0	97
60	40	1:2.8	93	100	50	1:2.0	94
60	50	1:3.5	96	100	60	1:2.5	92
60	60	1:4.0	97	100	80	1:3.3	92
60	80	1:5.5	92	100	100	1:4.0	97

must be true in the case of BPMG-Zn(II) combination also, as the log K_s value of the complex between BPMG and Zn^{2+} is 14.46 (Sawada et al., 2000), which is in between the log K_s values for AMP-Zn^{2+} complex and HEDP-Zn^{2+} complex. At low pH values <5, the protonation of ligand is greater, which is not favorable for the complex formation, and at pH (9, there is interference of OH^- ions in the complexation of phosphonate with Zn(II) (Deluchat et al., 1997). In the present study, the minimum concentrations of BPMG and Zn^{2+} corresponding to the highest IE of 95% are 1.5×10^{-4} M and 4.6×10^{-4} M respectively. That means that a much higher concentration of Zn^{2+} than BPMG is required to afford the highest IE. This can be explained as follows:

The complexation equilibrium between Zn^{2+} ions and BPMG can be written as:

$$Zn^{2+} + [HL]^{4-} \rightleftarrows [Zn\text{-}HL]^{2-} \text{ complexed species} \tag{4}$$

where $[HL]^{4-}$ indicates the ligand, which may exist as

$$^{-2}O_3P - CH_2 - \overset{+}{N}H(CH_2COO^-) - CH_2 - PO_3^{2-}$$

Carter et al. (1967) studied the acidity constants and complexation of Ca^{2+} and Mg^{2+} with nitrilotri(methylenephosphonic acid) (NTMP) and its N-oxide. They reported that pK_1 and pK_2 values of NTMP as well as its N-oxide are less than 2. This indicates the easy deprotonation from any two –OH groups of phosphonate moieties present in these compounds. Menelaou et al. (2009) reported studies on binary Ni(II)-(carboxy)phosphonate systems. In their studies, they structurally characterized the complex of N-(phosphonomethyl) glycine (H_3IDAP) with Ni^{2+} obtained at pH 4. They reported that the complex consists of the ligand, represented as $HIDAP^{2-}$, formed after the deprotonation from –COOH group and nitrogen. Mateescu et al. (2007) studied the structural characterization of an assembly of species between Co(II) and BPMG (H_5L). They inferred that the structure of Co-BPMG complex obtained at pH 5.5 consists BPMG in the form of $[HL]^{4-}$ as well as L^{5-}. Based on all these literature reports, it can be concluded that at pH 7 maintained during the gravimetric measurements in the present study, BPMG can be denoted as $[HL]^{4-}$. The K_s value of the complex may be represented by

$$K_s = [[Zn\text{-}HL]^{2-}]/[Zn^{2+}][[HL]^{4-}] \tag{5}$$

When the concentration of Zn^{2+} is much higher, the equilibrium (4) is shifted towards the right and the concentration of the $[Zn\text{-}BPMG]^{2-}$ complex increases. Sufficient concentration of this complex is necessary for it to get attached to the metal surface at anodic sites. Second, there will be enough concentration of free zinc ions at the molar ratio of $[BPMG]/[Zn^{2+}]$ of 1:3. It is also necessary that free zinc ions from the solution diffuse to the metal surface and precipitate an optimum amount of zinc hydroxide at the cathodic sites.

The influence of pH on the IE values of various compositions of the BPMG-Zn^{2+} system, which showed IE > 90% at pH 7, is shown in Figure 3. No adverse effect on the IE is observed with a decrease of pH from 7.0 to 5.0. When the pH was decreased from 5.0 to 4.0, no formulation was found to be effective in corrosion inhibition.

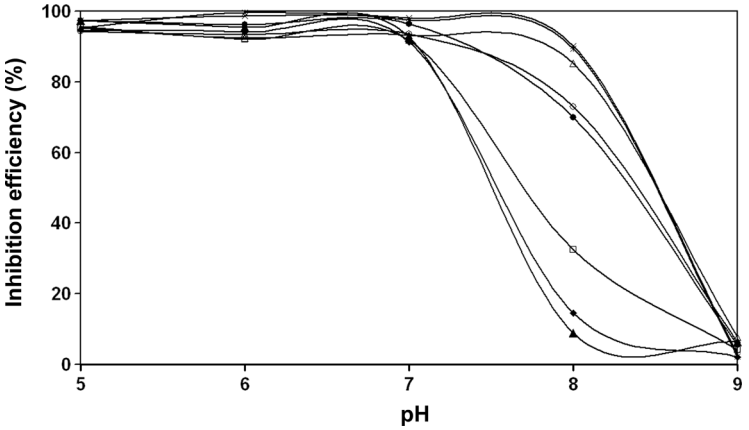

Figure 3. Corrosion inhibition efficiency of various binary inhibitor formulations as a function of pH: —■—BPMG (40 ppm) + Zn^{2+} (40 ppm); —□—BPMG (40 ppm) + Zn^{2+} (50 ppm); —▲—BPMG (40 ppm) + Zn^{2+} (60 ppm); —⊖—BPMG (60 ppm) + Zn^{2+} (40 ppm); —●—BPMG (60 ppm) + Zn^{2+} (50 ppm); —⋇—BPMG (60 ppm) + Zn^{2+} (60 ppm); —△—BPMG (80 ppm) + Zn^{2+} (40 ppm); —✳—BPMG (80 ppm) + Zn^{2+} (50 ppm).

When the pH was increased from 7.0 to slightly alkaline, say 8.0, the IE was slightly decreased. However, a few combinations offered a maximum IE of 95% even at pH 8. But when the pH is further increased to 9.0, none of the binary formulations showed good IE. The reasons for decrease in IE in more alkaline and more acidic environments are explained under the mechanistic aspects.

Electrochemical Impedance Studies

Nyquist plots for carbon steel immersed in 200 ppm of NaCl solution at pH 7 in the absence and presence of various formulations are shown in Figure 4. In case of the control as well as in the presence of various formulations, the Nyquist plots are found to be depressed semicircles instead of ideal semicircles. This kind of phenomenon is

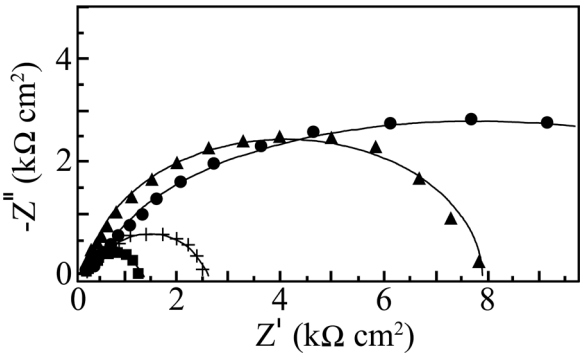

Figure 4. Nyquist plots for carbon steel in various aqueous environments: + NaCl (200 ppm); ▲ NaCl (200 ppm) + BPMG (40 ppm); ■ NaCl (200 ppm) + Zn^{2+} (30 ppm); ● NaCl (200 ppm) + BPMG (40 ppm) + Zn^{2+} (30 ppm) (the lines show the fitted curves).

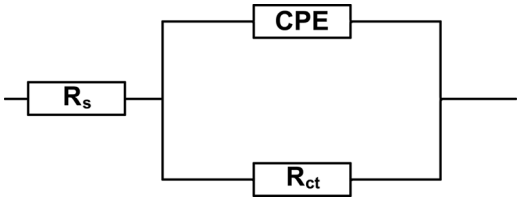

Figure 5. The equivalent circuit used to fit the impedance spectra.

called the dispersing effect (Li et al., 1998). When the complex plane impedance contains a depressed semicircle with its center below the real axis, which is characteristic for solid electrodes, it is often attributed to roughness and inhomogeneities of the solid surface (Juttner, 1990). It is also attributed to the distribution of active sites, adsorption of inhibitor molecules, and formation of porous layers (El Hosary et al., 1972). In such cases, the parallel network charge transfer resistance-double layer capacitance ($R_{ct} - C_{dl}$) is a poor approximation, especially for systems where an efficient inhibitor is present. Due to the fact that the double layer does not behave as an ideal capacitor in the presence of the dispersing effect, a constant phase element (CPE) is substituted for the capacitor to fit the impedance behavior of the electrical double layer more accurately (Mansfeld et al., 1985; Gunasekaran and Chauhan, 2004; Morad, 2000; Wu et al., 1999). CPE can thus be regarded as a nonideal capacitance (Scheider, 1975). The admittance and impedance of a CPE are, respectively, defined as

$$Y_{CPE} = Y_o\ (j\omega)^n$$

$$Z_{CPE} = A\ (j\omega)^{-n}$$

where ω is the angular frequency, Y_o is the modulus, which represents different quantities, depending on the value of CPE exponent, n, and A is the proportional factor, which is the reciprocal of modulus (Gunasekaran and Chauhan, 2004; Morad, 2000; Wu et al., 1999; Ma et al., 1997). For a highly polished electrode, the value of n is close to 1.0. The lower the value of n, the rougher the electrode surface. It can be seen that when $n = 1$, the element CPE becomes an ideal capacitor. The value of n is also related to the inherent physical and chemical heterogeneous nature of the solid surface, the presence of a porous corrosion product layer, and nonuniform distribution of current density on the surface (Olivares-Xometl et al., 2009; Touzet et al., 1993; Macdonald and McKubre, 1982).

All the Nyquist plots obtained in the present study are characterized by single time constant. The experimental data obtained from these plots are fitted by the equivalent electrical circuit shown in Figure 5. Such an equivalent circuit was also discussed by several researchers (Gunasekaran and Chauhan, 2004; Morad, 2000; Alagta et al., 2007), who obtained similar depressed semicircles with single time constant. The impedance parameters, charge transfer resistance (R_{ct}), constant phase element (CPE), and CPE exponent (n), obtained from the Nyquist plots and the calculated inhibition efficiency (IE_i) values are shown in Table II. Charge transfer resistance (R_{ct}) and the nonideal capacitance (CPE) are the two important parameters related to corrosion processes at the metal/solution interface. The former

Table II. Impedance parameters for carbon steel in 200 ppm NaCl environment in the absence and presence of inhibitor formulation

Concentration (ppm)		Impedance parameters			
BPMG	Zn^{2+}	Charge transfer resistance, R_{ct} (Ω cm^2)	Constant phase element, CPE (μF/cm^2)	CPE exponent, n	IE_i (%)
0	0	2575	13.41	0.592	—
40	0	7810	9.77	0.631	67.03
0	30	1150	21.54	0.713	—
40	30	17469	7.52	0.863	85.26
60	0	8003	8.54	0.580	67.82
0	50	1321	20.11	0.701	—
60	50	16511	4.18	0.813	84.40
60	0	8003	8.54	0.580	67.82
0	60	1371	18.63	0.731	—
60	60	16098	2.23	0.811	84.00

is directly related to the rate of corrosion reaction at the interface, while the latter is related to the structure of the electrical double layer at the interface. During corrosion inhibition by the adsorption of inhibitor molecules, high R_{ct} values can be obtained due to the slower corroding system (Babic-Samardzija et al., 2005; Khaled, 2003). Consequently, the decrease in CPE can result from the decrease of the local dielectric constant and/or from the increase of the thickness of the electrical double layer, which suggests an adsorption of the inhibitor molecules on the metal surface (Machnikova et al., 2008). Hence, for an effective inhibition process, there will be an increase in R_{ct} and decrease in CPE. However, there are inhibition processes that are associated with increase in capacitance values. This can be interpreted as due to the replacement of water molecules in the interface by ionic inhibitor species and/or due to oxides/hydroxides of metal formed due to initial corrosion. Bonnel et al. (1983) studied corrosion of carbon steel in neutral chloride solution by the impedance technique. They obtained high capacitance values in their studies and ascribed them to the existence of a layer of inner corrosion products.

In the present study, in the presence of the control alone, a small semicircle with an R_{ct} value of 2575 Ω is observed. A similar semicircle is also obtained when 30 ppm of Zn^{2+} is added to the control. Due to Zn^{2+} ions, R_{ct} is decreased and CPE value is increased with a slight increase in the value of n. These changes are due to the replacement of water molecules in the interface by zinc ions, which resulted in the increased rate of corrosion. By the addition of 40 ppm of BPMG to the control, a single and slightly depressed semicircle with high R_{ct} value is obtained. The capacitance value is decreased and n value is increased. These observations can be attributed to the presence of organic inhibitor molecules in the double layer and the control of corrosion processes to some extent. When the combination of 40 ppm of BPMG and 30 ppm of Zn^{2+} is considered in the presence of the control, a large depressed semicircle is observed from high frequency to low frequency regions in the Nyquist plot, indicating that the charge transfer resistance becomes dominant in the corrosion processes due to the presence of protective film on the metal surface.

This result is supported by the significant decrease in CPE and an increase in n value. The semicircle obtained in the presence of BPMG/Zn^{2+} represents an R_{ct} value of 17469 Ω, which is about six times greater than that observed in case of the control. The CPE value at the metal/solution interface is found to decrease from 13.41 μF cm^{-2} in the case of the control to 7.52 μF cm^{-2} in the case of the binary inhibitor formulation. This is because of the replacement of water molecules in the electrical double layer by the organic molecules having low dielectric constants (Wang et al., 2002). The value of n is considerably increased to 0.863 in the presence of the binary inhibitor system, suggesting a decrease of inhomogeneity of the interface during inhibition. Similar results are obtained from impedance studies in the case of other two binary inhibitor formulations, BPMG (60 ppm) + Zn^{2+}(50 ppm) and BPMG (60 ppm) + Zn^{2+} (60 ppm). The Nyquist plots obtained in the case of these formulations are not shown here. However, the data obtained from the plots are included in the Table II. All these results indicate that there is formation of a protective film in the presence of the binary inhibitor formulation. Several authors who studied the inhibitory effects of phosphonate-based corrosion inhibitors also reported that there is formation of thick and less permeable protective film on the metal surface (Felhosi et al., 1999; Gonzalez et al., 1996; Pech-Canul and Bartolo-Perez, 2004). They also concluded that the protective film consists of phosphonate-metal complexes. The impedance results of the present study also imply the synergistic action operating between BPMG and Zn^{2+}. This is in agreement with the inferences drawn from gravimetric studies.

Potentiodynamic Polarization Studies

The potentiodynamic polarization curves of carbon steel electrode in 200 ppm NaCl solution at pH 7 in the absence and presence of various inhibitor combinations are shown in Figure 6. The Tafel parameters derived from these curves and the inhibition efficiency values are listed in Table III. The corrosion potential (E_{corr}) in

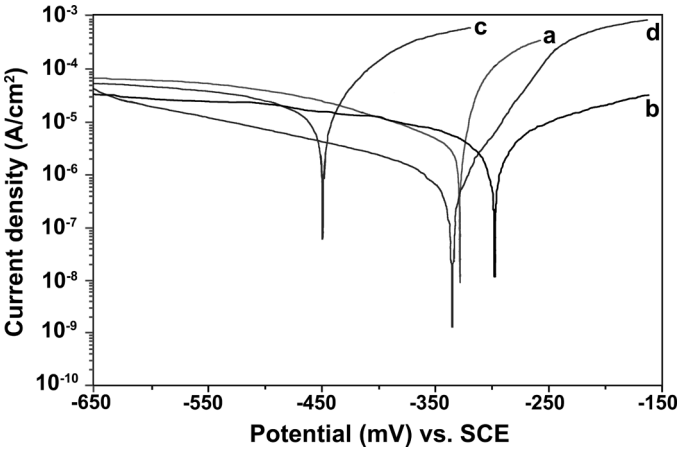

Figure 6. Potentiodynamic polarization curves for carbon steel in various aqueous environments: a, NaCl (200 ppm); b, NaCl (200 ppm) + BPMG (40 ppm); c, NaCl (200 ppm) + Zn^{2+} (30 ppm); d, NaCl (200 ppm) + BPMG (40 ppm) + Zn^{2+} (30 ppm).

Table III. Tafel parameters for carbon steel in 200 ppm NaCl environment in the absence and presence of inhibitor formulations

Concentration (ppm)		Tafel parameters				
BPMG	Zn^{2+}	E_{corr} (mV vs. SCE)	i_{corr} ($\mu A/cm^2$)	β_a (mV/decade)	β_c (mV/decade)	IE_p (%)
0	0	−323.4	12.84	45	132	—
40	0	−295.1	10.51	97	112	18.14
0	30	−447.8	13.63	41	117	—
40	30	−334.9	1.38	63	104	89.25
60	0	−281.5	11.23	109	105	12.53
0	50	−503.8	15.97	38	108	—
60	50	−357.1	1.24	71	97	90.34
60	0	−281.5	11.23	109	105	12.53
0	60	−523.3	17.03	35	102	—
60	60	−370.7	0.74	69	88	94.23

the case of the control is −323.4 mV versus SCE and the corresponding corrosion current density (i_{corr}) is 12.84 $\mu A/cm^2$. BPMG alone shifts the E_{corr} value to a more anodic side. In the presence of BPMG alone, decrease in anodic and cathodic current densities is observed. The i_{corr} value is reduced slightly to 10.51 $\mu A/cm^2$ in the presence of BPMG alone. The shift in anodic Tafel slope (β_a) is greater than the shift in cathodic Tafel slope (β_c) in the presence of 2-phosphobutane-1,2,4-tricarboxylic acid (PBTC) alone. According to the literature reports (Gonzalez et al., 1996; To et al., 1997), phosphonates in general are anodic inhibitors. When zinc ions alone are considered, the cathodic current density values are slightly reduced, while the anodic current densities are increased. The cathodic reaction is controlled by the formation of zinc hydroxide at cathodic sites. The corrosion potential is shifted to the cathodic side and the shift in cathodic Tafel slope is greater. Contrary to the result obtained in the case of BPMG, zinc ions increased the rate of corrosion as implied by increase in corrosion current density. Such an increase in corrosion rate in the presence of zinc ions alone was also reported in the literature (Rajendran et al., 2001). From the polarization curves shown in Figure 6, it is clear that the combination of BPMG (40 ppm) and Zn^{2+} (30 ppm) significantly decreased both the anodic and cathodic current density values when compared to the control. Thus, it is evident that this formulation acts as an effective mixed-type inhibitor. There is a slight shift in corrosion potential to a more cathodic side, and the shift in cathodic Tafel slope is greater than the shift in anodic Tafel slope. The corrosion current density is significantly decreased from 12.84 to 1.38 $\mu A/cm^2$, corresponding to an inhibition efficiency of 89.25%. Thus, the synergistic mixture of 40 ppm of BPMG and 30 ppm of Zn^{2+} is proved to be an effective corrosion inhibitor for carbon steel. This inference is also supported by similar results obtained when two more effective binary inhibitor formulations, BPMG (60 ppm) + Zn^{2+} (50 ppm) and BPMG (60 ppm) + Zn^{2+} (50 ppm), are considered for polarization studies. The results obtained in the case of these two formulations are given in Table III. All these results indicate that the binary inhibitor formulation retards both the anodic dissolution of carbon steel and oxygen reduction at cathodic sites in the corrosion inhibition process. Nevertheless, the

effect on cathodic reaction is more pronounced. Similar phosphonate-based formulations were reported to be mixed inhibitors (Gonzalez et al., 1996; Pech-Canul and Bartolo-Perez, 2004; Rajendran et al., 1999a).

A significant observation related to the inhibition efficiency values is to be noted. If the inhibition efficiency values obtained from gravimetric (IE_g), polarization (IE_p), and EIS (IE_i) studies are compared, slight differences are observed. It is suggested that the inhibition efficiency values obtained from various methods may not be strictly comparable when the immersion times used in these methods are not same.

X-ray Photoelectron Spectroscopic Studies (XPS)

The XPS deconvolution spectra of the individual elements, namely phosphorus, nitrogen, and zinc, present in the surface film formed in the control solution in the presence of the inhibitor formulation are shown in Figures 7 to 9. The deconvolution spectra of the elements Fe, O, and C obtained in the case of both the control and inhibitor are not included here. The interpretation of all these spectra is done with the help of the data of the elemental binding energies reported in the literature and also with the help of the reports published on the analysis of XPS spectra of the surface films.

The Fe 2p deconvolution spectrum in the case of the control contains two peaks, one at 710.8 eV corresponding to Fe $2p_{3/2}$ and the other one at 724.2 eV corresponding to the Fe $2p_{1/2}$ electron. The peak due to Fe $2p_{3/2}$ is interpreted for the determination of the chemical state of iron in the surface film. The peak of Fe $2p_{3/2}$ at 710.8 eV is the one, shifted from 707.0 eV, of the characteristic elemental binding energy of the Fe $2p_{3/2}$ electron (Moulder et al., 1995). Such a large shift of 3.8 eV suggests that iron is present in the Fe^{3+} state in the surface film. The presence of a peak due to Fe $2p_{3/2}$ observed in the case of the control at 710.8 eV can be ascribed to the presence of iron in the form of γ-Fe_2O_3, Fe_3O_4, and FeOOH (Pech-Canul and Bartolo-Perez, 2004; Kalman et al., 1994; McIntyre and Zetaruk, 1977; Maroie et al., 1979). The spectrum corresponding to the inhibitor system showed the Fe $2p_{3/2}$ peak

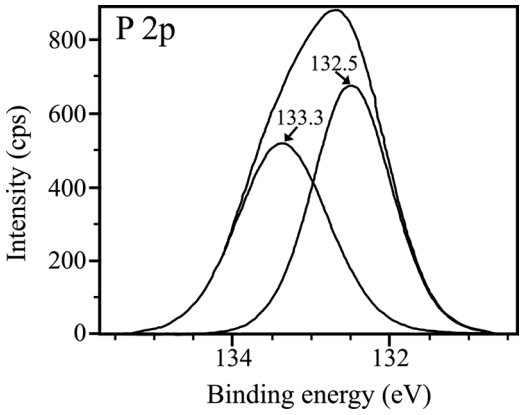

Figure 7. XPS deconvolution spectrum of P 2p in the surface film formed in the presence of the inhibitor formulation BPMG (40 ppm) + Zn^{2+} (30 ppm).

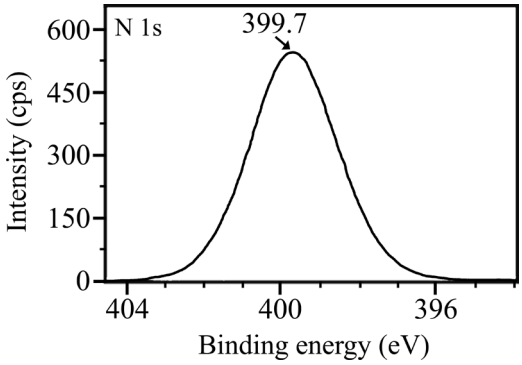

Figure 8. XPS deconvolution spectrum of N 1s in the surface film formed in the presence of the inhibitor formulation BPMG (40 ppm) + Zn^{2+} (30 ppm).

at 711.0 eV, and the peak at 724.8 eV is due to Fe $2p_{1/2}$. Thus, the Fe $2p_{3/2}$ peak obtained in the case of the inhibitor formulation implies the presence of oxides and hydroxides like Fe_2O_3, Fe_3O_4, and FeOOH and also involvement of Fe^{3+} in the complex formation with the inhibitor molecules. No peak is observed due to elemental iron in the case of both the control and the inhibitor formulation. This result implies the formation of thick films in both cases. The film is non-protective in the case of the control and less porous and highly protective in the presence of the inhibitor. If the intensities of Fe $2p_{3/2}$ peaks are compared, they are 4600 cps for control and only 400 cps for the inhibitor system. Such a large decrease in the intensity of the Fe 2p peak in the presence of the inhibitor formulation can be understood in terms of formation of protective film and consequently less corrosion of iron and less iron oxide. The binding energy of the Fe^{2+} state in iron oxides was reported to be around 708.5 eV (Asami et al., 1976). The absence of any peak in this region in the present study also supports that iron does not exist in the Fe^{2+} state.

The XPS spectrum of phosphorus is shown in Figure 7. Two P 2p peaks are observed, one each at 132.5 eV and 133.3 eV. They suggest the presence of BPMG

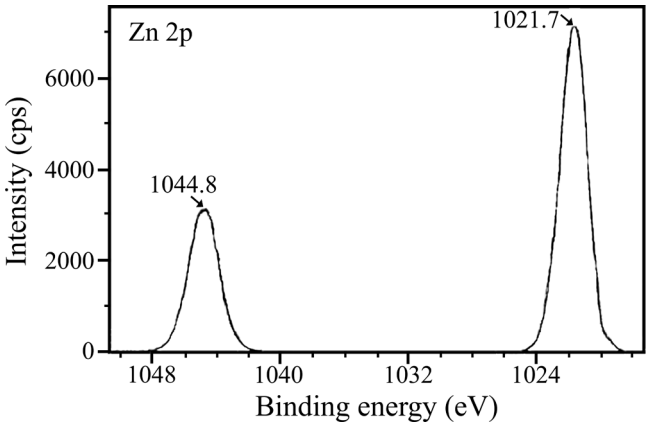

Figure 9. XPS deconvolution spectrum of Zn 2p in the surface film formed in the presence of the inhibitor formulation BPMG (40 ppm) + Zn^{2+} (30 ppm).

in the surface film formed in the presence of inhibitor formulation (Nakayama, 2000; Felhosi et al., 1999; Ochoa et al., 2002; Koudelka et al., 1982). Figure 8 shows the N 1s peak in the XPS spectrum of the surface film appeared at 399.7 eV, while the characteristic elemental binding energy of the N 1s electron is 398.0 eV (Moulder et al., 1995). That means there is a shift of 1.7 eV in the binding energy of the N 1s electron. This shift may be attributed to the presence of BPMG molecule in the surface film in the form of a complex with Fe(III) and Zn(II) (El Azhar et al., 2002; Meneguzzi et al., 1999). The C 1s spectrum in the case of the control showed a single peak at 284.6 eV. This peak is due to contamination from the vacuum system and chamber during the analysis (Cicileo et al., 1999). In the case of the inhibitor formulation, the C 1s spectrum has three peaks; one is the high intense peak at 284.4 eV and the other two are low intense peaks at 285.9 eV and 288.2 eV. BPMG has various carbon environments and hence the three peaks observed in the presence of the inhibitor formulation indicate the presence of BPMG in the surface film. The intensity of the C 1s peak in the presence of the inhibitor is about twice that of the peak in the case of the control. It supports the presence of BPMG in the surface film of the inhibited substrate. This interpretation can be supported from studies reported in the literature (Ochoa et al., 2002; Aramaki and Shimura, 2003; Gunasekaran and Chauhan, 2004).

In the case of the control, two peaks corresponding to O 1s are observed, one at 530.1 eV and the other at 533.0 eV. The latter peak is due to adsorbed water on the surface (Asami et al., 1976; Nakayama, 2000; Karman et al., 1998; Ochoa et al., 2002). The O 1s peak observed at 530.1 eV is due to O^{2-} (Karman et al., 1998; Pech-Canul and Bartolo-Perez, 2004). In the present study, the presence of O^{2-} in the surface film formed in the presence of the control may be in the form of oxides/hydroxides of Fe(III). In the case of the inhibitor formulation, a single O 1 s peak of high intensity was observed at 531.2 eV. This peak may be interpreted as follows. The XPS of surface film in the presence of the inhibitor showed that besides oxygen, there is the presence of carbon, nitrogen, phosphorus, iron, and zinc in the surface film. That means that BPMG is present on the surface, zinc is present as Zn^{2+}, and the interpretation given above in the case of Fe 2p indicates the presence of Fe_2O_3, Fe_3O_4, and FeOOH. Hence, the O 1 s peak observed in the inhibited surface film can be ascribed to the presence of $Zn(OH)_2$, Fe_2O_3, Fe_3O_4, FeOOH, and oxygen of BPMG in the surface film (Asami et al., 1976; Fang et al., 1993; Felhosi et al., 1999; Pech-Canul and Bartolo-Perez, 2004). The disappearance of the peak around 533 eV in the case of the inhibitor formulation indicates the absence of water molecules in the surface film, as they have been completely replaced by the inhibitor molecules.

Figure 9 presents the XPS deconvolution spectrum of zinc. The Zn $2p_{3/2}$ peak is observed at 1021.7 eV and the Zn $2p_{1/2}$ peak at 1044.8 eV. The Zn $2p_{3/2}$ peak is normally interpreted. The high intensity of the Zn $2p_{3/2}$ peak may be ascribed to the presence of $Zn(OH)_2$ in the surface film and also to the involvement of Zn^{2+} in the complex formation with BPMG (Felhosi et al., 1999; Aramaki, 2004).

Along with the elements discussed above, the survey spectrum (not shown) in the case of the control has a low intensity chlorine peak at 200.0 eV. This is because some chloride ions reach the metal surface and are responsible for corrosion of the metal. The chlorine peak is not observed in the survey spectrum of inhibited surface film, which indicates that the protective film does not allow the aggressive ions to reach the metal surface. After consolidating all the inferences drawn from the XPS of

individual elements present in surface films, it is suggested that the surface film consists of mainly [Zn(II)-BPMG] complex, $Zn(OH)_2$, and small amounts of oxides/hydroxides of Fe(III) in the case of the inhibitor system. The complex may be chemisorbed on the metal surface and get attached to the Fe(III) ions.

Interpretation of FT-IR Spectra

The reflection absorption FT-IR spectra of the surface films formed on carbon steel in the absence and presence of the inhibitor formulation are shown in Figure 10. The spectrum of the surface film in the presence of the inhibitor is interpreted by comparison with the FT-IR spectrum of pure BPMG (not presented here) as well as with the help of literature reports. In the FT-IR spectrum of BPMG, multiple bands in the region 900–1200 cm^{-1} were assigned to phosphonate group stretching frequencies. The peak at 1181 cm^{-1} can be assigned to $-PO_3$ antisymmetric (ν_{as}) stretching, while the peak at 1080 cm^{-1} is assigned to symmetric (ν_s) stretching of $-PO_3$. The peak observed at 933.5 cm^{-1} can be attributed to the P–OH stretching vibrations. In the case of the inhibited surface film, the antisymmetric and symmetric stretching vibrations $\nu_{as}(PO_3)$ and $\nu_s(PO_3)$ are observed in the form of a broad band between 1140 and 1050 cm^{-1}. The P–OH stretching located at 913.5 cm^{-1} is observed to be weak. These results can be interpreted in terms of interaction between $P\text{-}O^-$ present in the phosphonate with metallic species, Zn(II) and Fe(III), to form P–O–Zn and P–O–Fe bonds. This interpretation was also given by several authors who worked on corrosion inhibition of carbon steel by phosphonates (Gonzalez et al., 1996; To et al., 1997; Amar et al., 2008). Carter et al. (1986) found that FT-IR spectra obtained with an organic phosphonate on a steel substrate are consistent with the phosphonate reaction on steel to produce a metal salt. This also suggests that phosphonates are coordinated with metal ions, resulting in the formation of [metal-phosphonate] complexes on the metal surface.

A weak band observed around 1335 cm^{-1} indicates the presence of zinc hydroxide in the surface film (Gunasekaran et al., 1997; Sekine and Hirakawa, 1986; Amar

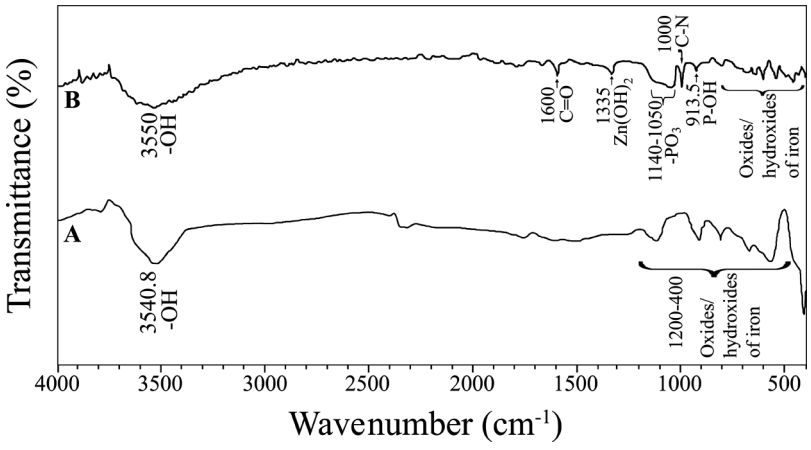

Figure 10. Reflection absorption FT-IR spectra of the surface films: A, control; B, inhibitor formulation BPMG (40 ppm) + Zn^{2+} (30 ppm).

et al., 2008). An intense band at 1732 cm^{-1} in the FT-IR spectrum of BPMG is the characteristic of uncoordinated, protonated carboxylate carbonyl group in BPMG. In the case of the inhibited surface film, this band is observed at 1600 cm^{-1}. It indicates the presence of BPMG molecules in the surface film. The shift in the absorption frequency is due to involvement of the phosphonate in complexation with metal ions. A band at 1000 cm^{-1} is due to C–N stretching vibration shifted from 1157 cm^{-1} observed in the case of pure BPMG. The shift towards lower wave number indicates the formation of a coordinate bond between metal ions and phosphonate molecule. There are several bands in the region 1200–400 cm^{-1} in both spectra of surface films. Many of these peaks imply the presence of various oxides and hydroxides of iron like Fe_3O_4, FeOOH, and Fe_2O_3 (Nakayama, 2000; Aramaki and Shimura, 2003). Shi Yu and Gan Moog Chow (2004) obtained peaks at 570 cm^{-1} and 630 cm^{-1} and assigned them to amorphous oxides of Fe_2O_3 and Fe_3O_4. Amar et al. (2008) obtained absorption peaks between 750 and 1100 cm^{-1} in the spectra of metal surfaces in the presence of 3% NaCl solution. They ascribed them to corrosion products of ferric hydroxide (γ-FeOOH) and magnetite (Fe_3O_4). A moderately intense and a broad band formed at 3540.8 cm^{-1} in the case of the control can be assigned to the presence of –OH group on the surface. This hydroxyl group may be in the form of FeOOH and/or $Fe(OH)_3$ (Bellamy, 1968). Such a peak is also observed in the spectrum of the inhibited surface film. This peak can be assigned to the –OH groups present in the inhibitor molecule, to $Zn(OH)_2$, and a small contribution of hydroxide of Fe(III) present in the inhibited film. Thus, the reflection absorption FT-IR spectrum of the surface film formed in the presence of the inhibitor formulation implies the presence of [Zn(II)-BPMG] complex, $Zn(OH)_2$, and small amounts of oxides and hydroxides of Fe(III).

The XPS spectra and the reflection absorption FT-IR spectrum of the surface film imply the presence of Fe(III), Zn(II), and BPMG in the surface film. The shifts in binding energies of various elements and shifts in the absorption band frequencies of various functional groups implied that BPMG is involved in the complex formation with Zn^{2+} and Fe^{3+}. This inference is further supported by several studies reported in literature. Pilbath et al. (2008a,b, 2009) studied corrosion protection of zinc using diphosphonate thin films. In their studies, they concluded that the surface film formed after the treatment with diphosphonate consists of an insoluble zinc-phosphonate compound layer, which is responsible for protection of zinc from corrosion. Demadis et al. (2006) investigated the structure of calcium-2-phosphonobutane-1,2,4-tricarboxylic acid (Ca-PBTC) complex obtained by the reaction of $CaCl_2 \cdot 2H_2O$ and PBTC in a 1:1 molar ratio. Holm et al. (1989) studied the nature of the film formed on carbon steel in cooling water in the presence of an inhibitor containing 20 ppm of 2-phosphobutane-1,2,4-tricarboxylic acid (PBTC) and 200 ppm of Ca^{2+} ions by XPS and atomic emission spectroscopy (AES) techniques. They concluded that PBTC is present as deprotonated Ca(II)-PBTC complex, which reacts with the Fe(III) ions at the steel surface to form cross-linked, amorphous, anhydrous Fe(III)-Ca(II)-PBTC compound. Mao and Clearfield (2002) synthesized a ternary zinc complex with a phosphonic acid, namely N-(phosphonomethyl) iminodiacetic acid (PMIDA), and a carboxylic acid, namely acetic acid. They reported that the crystal structure of that complex, $Zn_2(PMIDA)(CH_3COOH) \cdot 2H_2O$, features a two-dimensional zinc carboxylate-phosphonate hybrid layer.

Kuznetsov (2003) reported that the mechanism of action of phosphonates is not only associated with adsorption but also with electrophilic substitution of

complex-forming surface cations, precipitation of almost insoluble hydroxides, and formation of hetero- and polynuclear complexes. Freedman (1984) reported in his study on cooling water systems that although the key role of zinc ions in corrosion inhibition is to precipitate zinc hydroxide on the metal surface, in some cases, the zinc ions also complex with the stabilizing agents. Shaban et al. (1993) studied the inhibitive effect of N-phosphonomethyl glycine (NPMG) on corrosion of steel. One of their interpretations was that Ca^{2+} and Zn^{2+} ions form a passivating complex with NPMG on the steel surface, which protects the metal. Felhosi et al. (1999) studied the effects of bivalent cations on corrosion inhibition of steel by HEDP. They interpreted their XPS results in terms of formation of complex between HEDP and Zn^{2+} on the carbon steel surface. They mentioned that there is formation of heteropolynuclear complexes on the iron surface. Gonzalez et al. (1996) studied the synergistic effect between amino-trimethyl phosphonic acid (ATMP) and zinc chloride in corrosion inhibition of carbon steel with 0.5 M NaCl as the control. They reported that ATMP forms chelate compounds with Zn^{2+} and Fe^{3+}, and this leads to the enhancement of corrosion protection due to construction of a dense system that prevents the penetration of aggressive species. Demadis et al. (2005b) reported the anticorrosion effects of zinc-hexamethylenediaminetetrakis(methylenephosphonate) (Zn-HDTMP) on carbon steels. They concluded that the corrosion protection of carbon steel in the presence of Zn^{2+} and HDTMP is due to Zn-HDTMP complex. Based on all these literature reports on various phosphonates and the requirement of optimum concentration of zinc ions for effective inhibition and also on the high intensity Zn 2p peaks obtained from XPS spectrum, it can be inferred that Zn(II) and Fe(III) are involved in the complex formation with BPMG to form [Fe(III), Zn(II)-BPMG] polynuclear complex, which plays a significant role in making the surface film protective.

Surface Analysis by SEM

Figure 11 shows the high resolution SEM images of the surfaces of carbon steel immersed for seven days in the control in the absence and presence of the inhibitor, BPMG (40 ppm) + Zn^{2+} (30 ppm). Figure 11A reveals that the surface is severely corroded and there is formation of different forms of corrosion products (iron oxides) on the surface in the absence of the inhibitor. The entire surface is covered by a scale-like black corrosion product on which there is growth of another corrosion product appearing in the form of white clusters at several sites. A very few of such clusters are shown at the submicron level in Figure 11B. Figures 11C and 11D show the morphological features of the inhibited surface. The corrosion product deposits observed in the case of the control are not present on the inhibited surface. It indicates that the penetration of Cl^- ions of the environment onto the substrate is controlled effectively through good surface coverage by the inhibitor film. The higher magnification ($\times$5000) SEM image (Figure 11D) of the inhibited surface shows some low-depth inhomogeneities on the surface. But a closer look at such sites reveals that the inhomogeneities are due to the structural defects of the metal substrate and that these sites are also covered by the inhibitor film. Thus, the inhibitor film covers the entire metal surface. This observation also accounts for the high inhibition efficiency values obtained during the gravimetric studies of the inhibitor system. From the SEM analysis it can be inferred that the inhibitor film exhibits good protective properties for carbon steel in low chloride media.

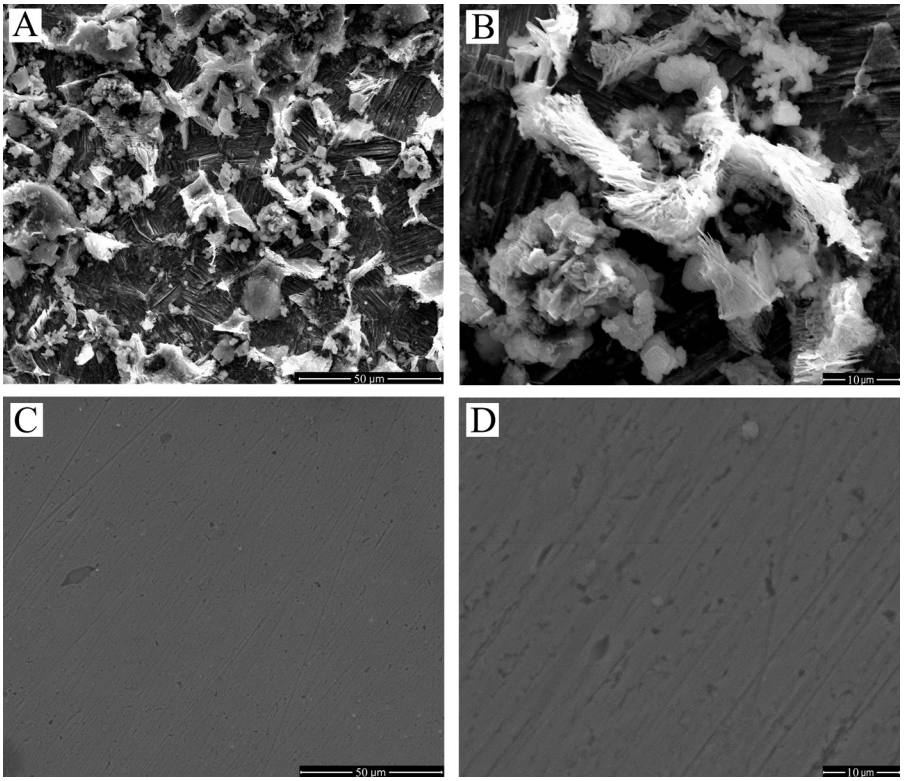

Figure 11. High-resolution SEM images of carbon steel surfaces after immersion in the control in the absence and presence of inhibitor for seven days: A and B, control, C and D, inhibitor. A and C magnification ×1000, B and D magnification ×5000.

Mechanism of Corrosion Protection

In order to explain all the experimental results, a plausible mechanism of corrosion inhibition is proposed as follows:

1. The mechanism of corrosion of carbon steel in nearly neutral aqueous media is well established. The well-known reactions are given below.

$$\mathrm{Fe} \longrightarrow \mathrm{Fe}^{2+} + 2\mathrm{e}^{-} \tag{6}$$

Fe^{2+} further undergoes oxidation in the presence of oxygen available in the aqueous solution.

$$\mathrm{Fe}^{2+} \xrightarrow{[\mathrm{O}_2]} \mathrm{Fe}^{3+} + \mathrm{e}^{-} \tag{7}$$

The corresponding reduction reaction at cathodic sites in neutral and alkaline media is

$$\mathrm{O}_2 + 2\mathrm{H}_2\mathrm{O} + 4\mathrm{e}^{-} \longrightarrow 4\,\mathrm{OH}^{-} \tag{8}$$

Fe^{3+} ions produced at anodic areas and OH^- ions produced at cathodic areas combine to form $Fe(OH)_3$, ($Fe_2O_3 \cdot H_2O$), which is precipitated on the surface of the metal due to its very low solubility product (K_{sp} of $Fe(OH)_3 = 1.1 \times 10^{-36}$).

2. When BPMG and Zn^{2+} ions are added to the aqueous solution, BPMG reacts with Zn^{2+} to form a binary complex, [Zn^{2+}-BPMG]. It diffuses to the metal surface and binds to Fe(III) ions present on the surface. The cross-linkage and reorganization of such complex ions on the surface will produce a polymeric network structure. The resulting polynuclear complex, [Fe(III), Zn(II)-BPMG], covers the anodic sites and controls the corresponding anodic reaction.

$$[\text{Zn(II)-BPMG}] + Fe^{3+} \longrightarrow [\text{Fe(III), Zn(II)} - \text{BPMG}] \tag{9}$$

3. Free Zn^{2+} ions are available in the bulk of the solution because of relatively higher molar concentration of Zn^{2+} in the inhibitor mixture. These Zn^{2+} ions diffuse to the metal surface and react with OH^- ions produced at the cathodic sites to form a precipitate of $Zn(OH)_2$.

$$Zn^{2+} + 2\,OH^- \longrightarrow Zn(OH)_2 \tag{10}$$

The precipitate of $Zn(OH)_2$ ($K_{sp} = 1.8 \times 10^{-14}$) is deposited on the cathodic sites and controls the cathodic partial reaction of the corrosion process.

4. The inhibitor formulation is effective in the pH range 5–8. At pH 9, higher concentrations of OH^- ions are available both in the bulk of the solution and on the surface. In such an environment, there is greater interference of OH^- ions in the complexation (Deluchat et al., 1997), leading to the formation of [Zn(II)-BPMG-OH] complex, which may not contribute to the formation of protective film on the metal surface. In acidic medium at $pH \leq 4$, the ligands will be in the protonated form and do not coordinate with Zn(II) as effectively as the deprotonated ligands. Second, enough $Zn(OH)_2$ will not be formed on the cathodic sites. Hence, the inhibitor is not effective at $pH \leq 4$.
5. Thus, BPMG and Zn^{2+} play a very important role in the synergistic effect in controlling corrosion through the formation of protective film on the metal surface. It is inferred that the film may consist of various oxides/hydroxides like Fe_2O_3, $Fe_3O_4 \cdot H_2O$, FeOOH, $Zn(OH)_2$, and a polynuclear complex, [Fe(III), Zn(II)-BPMG]. Each of these constituents contributes to make the film highly protective.

Conclusions

1. The binary system BPMG-Zn^{2+} is an effective corrosion inhibitor for carbon steel in low chloride aqueous environment. The strong synergistic effect between BPMG and Zn^{2+} is established through the present study.
2. The inhibitor formulation is effective in the pH range 5 to 8, which is generally applicable for cooling water systems.
3. Electrochemical impedance studies indicated the significant modification of the metal/solution interface by the formation of a dense and protective film in the presence of the inhibitor formulation.
4. The inhibitor mixture acts as a mixed-type inhibitor controlling both the anodic and cathodic reactions.

5. The protective film is composed of mainly [Zn(II)-BPMG] complex, $Zn(OH)_2$, and small amounts of oxides/hydroxides of Fe(III). The presence of optimum amounts of all these components is required at a given pH value to make the surface film protective.

References

Alagta, A., Felhosi, I., Telegdi, J., Bertoti, I., and Kalman, E. (2007). Effect of metal ions on corrosion inhibition of pimeloyl-1,5-di-hydroxamic acid for steel in neutral solution, *Corros. Sci.*, **49**, 2754–2766.

Amar, H., Benzakour, J., Derja, A., Villemin, D., and Moreau, B. (2003). A corrosion inhibition study of iron by phosphonic acids in sodium chloride solution, *J. Electroanal. Chem.*, **558**, 131–139.

Amar, H., Braisaz, T., Villemin, D., and Moreau, B. (2008). Thiomorpholin-4-ylmethyl-phosphonic acid and morpholin-4-methyl-phosphonic acid as corrosion inhibitors for carbon steel in natural seawater, *Mater. Chem. Phys.*, **110**(1), 1–6.

Aramaki, K. (2004). Preparation of self-healing protective films on a zinc electrode treated in a cerium(III) nitrate solution and modified with sodium phosphate and cerium(III) nitrate, *Corros. Sci.*, **46**, 1565–1579.

Aramaki, K., and Shimura, T. (2003). Prevention of passive film breakdown on iron in a borate buffer solution containing chloride ion by coverage with a self-assembled monolayer of hexadecanoate ion, *Corros. Sci.*, **45**, 2639–2655.

Asami, K., Hashimoto, K., and Shimodaira, S. (1976). X-ray photoelectron spectrum of Fe^{2+} state in iron oxides, *Corros. Sci.*, **16**, 35–45.

ASTM Standard G31-72. (2004). Standard practice for laboratory immersion corrosion testing of metals, ASTM International, West Conshohocken, Penn., DOI: 10.1520/G0031-72R04.

Awad, H. S. (2005a). The effect of zinc-to-HEDP molar ratio on the effectiveness of zinc-1, hydroxyethylidene-1,1 diphosphonic acid in inhibiting corrosion of carbon steel in neutral solutions, *Anti-corros. Methods Mater.*, **52**, 22–28.

Awad, H. S. (2005b). Surface examination and analysis of steel inhibited by 1-hydroxyethylidene-1,1-diphosphonic acid in presence of zinc ions, *Corros. Eng. Sci. Technol.*, **40**, 57–64.

Awad, H. S., and Turgoose, S. (2004). Influence of hardness salts on the effectiveness of zinc-1 hydroxyethylidene 1,1 diphosphonic acid (HEDP) mixtures in inhibiting the corrosion of mild steel in neutral oxygen-containing solutions, *Corrosion*, **60**, 1168–1175.

Babic-Samardzija, K., Lupu, C., Hackerman, N., Barron, A. R., and Luttge, A. (2005). Inhibitive properties and surface morphology of a group of heterocyclic diazoles as inhibitors for acidic iron corrosion, *Langmuir*, **21**, 12187–12196.

Bellamy, L. J. (1968). *Advances in Infrared Group Frequencies*, Methuen, London.

Bonnel, A., Dabosi, F., Deslouis, C., Duprat, M., Keddam, M., and Tribollet, B. (1983). Corrosion study of a carbon steel in neutral chloride solutions by impedance techniques, *J. Electrochem. Soc.*, **130**, 753–761.

Carter, R. O., Gierczak, C. A., and Dickie, R. A. (1986). The chemical interaction of organic materials with metal substrates. Part II: FT-IR studies of organic phosphate films on steel, *Appl. Spectrosc.*, **40**, 649–655.

Carter, R. P., Crutchfield, M. M., and Irani, R. R. (1967). Nitrilotri(methylenephosphonic acid) N-oxide and nitrilotriacetic acid N-oxide: Acidity and complexing of calcium and magnesium ions, *Inorg. Chem.*, **6**, 943–946.

Choi, D.-J., You, S.-J., and Kim, J.-G. (2002). Development of an environmentally safe corrosion, scale and microorganism inhibitor for open recirculating cooling systems, *Mater. Sci. Eng. A*, **335**, 228–235.

Cicileo, G. P., Rosales, B. M., Varela, F. e., and Vilche, J. R. (1999). Comparative study of organic inhibitors of copper corrosion, *Corros. Sci.*, **41**(7), 1359–1375.

Deluchat, V., Bollinger, J.-C., Serpaud, B., and Caullet, C. (1997). Divalent cations speciation with three phosphonate ligands in the pH-range of natural waters, *Talanta*, **44**, 897–907.

Demadis, K. D., Katarachia, S. D., and Koutmos, M. (2005a). Crystal growth and characterization of zinc–(amino-tris-(methylenephosphonate) organic-inorganic hybrid networks and their inhibiting effect on metallic corrosion, *Inorg. Chem. Commun.*, **8**, 254–258.

Demadis, K. D., Mantzaridis, C., Raptis, R. G., and Mezei, G. (2005b). Metal–organotetraphosphonate inorganic–organic hybrids: Crystal structure and anticorrosion effects of zinc hexamethylenediaminetetrakis(methylenephosphonate) on carbon steels, *Inorg. Chem.*, **44**, 4469–4471.

Demadis, K. D., Lykoudis, P., Raptis, R. G., and Mezei, G. (2006). Phosphonopolycarboxylates as chemical additives for calcite scale dissolution and metallic corrosion inhibition based on a calcium-phosphonotricarboxylate organic-inorganic hybrid, *Cryst. Growth Des.*, **6**, 1064–1067.

El Azhar, M., Traisnel, M., Mernari, B., Gengembre, L., Bentiss, F., and Lagrenee, M. (2002). Electrochemical and XPS studies of 2,5-bis(n-pyridyl)-1,3,4-thiadiazoles adsorption on mild steel in perchloric acid solution, *Appl. Surf. Sci.*, **185**, 197–205.

El Hosary, A. A., Saleh, R. M., and Shams El Din, A. M. (1972). Corrosion inhibition by naturally occurring substances – I. The effect of Hibiscus subdariffa (karkade) extract on the dissolution of Al and Zn, *Corros. Sci.*, **12**, 897–904.

Elachouri, E., Hajji, M. S., Salem, M., Kertit, S., Aride, J., Coudert, R., and Essassi, E. (1996). Some nonionic surfactants as inhibitors of the corrosion of iron in acid chloride solutions, *Corrosion*, **52**, 103–108.

Fang, J. L., Li, Y., Ye, X. R., Wang, Z. W., and Liu, Q. (1993). Passive films and corrosion protection due to phosphonic acid inhibitors, *Corrosion*, **49**, 266–270.

Felhosi, I., Keresztes, Zs., Karman, F. H., Mohai, M., Bertoti, I., and Kalman, E. (1999). Effects of bivalent cations on corrosion inhibition of steel by 1-hydroxyethane-1,1-diphosphonic acid, *J. Electrochem. Soc.*, **146**, 961–969.

Freedman, A. J. (1984). Cooling water technology in the 1980s, *Mater. Perform.*, **23**, 9–16.

Freeman, R. A., and Silverman, D. C. (1992). Error propagation in coupon immersion tests, *Corrosion*, **48**, 463–466.

Gonzalez, Y., Lafont, M. C., Pebere, N., and Moran, F. (1996). A synergistic effect between zinc salt and phosphonic acid for corrosion inhibition of a carbon steel, *J. Appl. Electrochem.*, **26**, 1259–1265.

Gunasekaran, G., and Chauhan, L. R. (2004). Eco friendly inhibitor for corrosion inhibition of mild steel in phosphoric acid medium, *Electrochim. Acta*, **49**, 4387–4395.

Gunasekaran, G., Palaniswamy, N., Appa Rao, B. V., and Muralidharan, V. S. (1997). Synergistic inhibition in low chloride media, *Electrochim. Acta*, **42**, 1427–1434.

Holm, R., Holtkamp, D., Kleinstuck, R., Rother, H.-J., and Storp, S. (1989). Surface analysis methods in the investigation of corrosion inhibitor performance, *Fresenius' Z. Anal. Chem.*, **333**, 546–554.

Jaworska, J., Genderen-Takken, H. V., Hanstveit, A., Plassche, E., and Feijtel, T. (2002). Environmental risk assessment of phosphonates, used in domestic laundry and cleaning agents in the Netherlands, *Chemosphere*, **47**, 655–665.

Juttner, K. (1990). Electrochemical impedance spectroscopy (EIS) of corrosion processes on inhomogeneous surfaces, *Electrochim. Acta*, **35**, 1501–1508.

Kalman, E., Karman, F. H., Telegdi, J., Varhegyi, B., Balla, J., and Kiss, T. (1993). Inhibition efficiency of N-containing carboxylic and carboxy-phosphonic acids, *Corros. Sci.*, **35**, 1477–1482.

Kalman, E., Karman, F. H., Cserny, I., Kover, L., Telegdi, J., and Varga, D. (1994). The effect of calcium ions on the adsorption of phosphonic acid: A comparative investigation with emphasis on surface analytical methods, *Electrochim. Acta*, **39**, 1179–1182.

Karman, F. H., Felhosi, I., Kalman, E., Cserny, I., and Kover, L. (1998). The role of oxide layer formation during corrosion inhibition of mild steel in neutral aqueous media, *Electrochim. Acta*, **43**, 69–75.

Khaled, K. F. (2003). The inhibition of benzimidazole derivatives on corrosion of iron in 1 M HCl solutions, *Electrochim. Acta*, **48**, 2493–2503.

Koudelka, M., Sanchez, J., and Augustynski, J. (1982). On the nature of surface films formed on iron in aggressive and inhibiting polyphosphate solutions, *J. Electrochem. Soc.*, **129**, 1186–1191.

Kuznetsov, Yu. I. (2003). New problems and possibilities of inhibition of corrosion of metals, paper 320 presented at The European Corrosion Congress (EUROCORR 2003), Budapest, Hungary, 28 September–2 October.

Li, S. L., Ma, H. Y., Lei, S. B., Yu, R., Chen, S. H., and Liu, D. X. (1998). Inhibition of copper corrosion with Schiff base derived from 3-methoxysalicylaldehyde and O-phenyldiamine in chloride media, *Corrosion*, **54**, 947–954.

Ma, H., Chen, S., Chen, X., Li, G., and Yang, X. (1997). Analysis of impedance data with dispersing effect by using the linear least squares regression method, *J. Serb. Chem. Soc.*, **62**, 1201–1212.

Macdonald, D. D., and McKubre, M. C. H. (1982). Impedance measurements in electrochemical systems, in: *Modern Aspects of Electrochemistry*, eds. J. O'M. Bockris, B. E. Conway, and R. E. White, Plenum Press, New York.

Machnikova, E., Whitmire, K. H., and Hackerman, N. (2008). Corrosion inhibition of carbon steel in hydrochloric acid by furan derivatives, *Electrochim. Acta*, **53**, 6024–6032.

Mansfeld, F., Kendig, M. W., and Lorenz, W. J. (1985). Corrosion inhibition in neutral, aerated media, *J. Electrochem. Soc.*, **132**, 290–296.

Mao, J.-G., and Clearfield, A. (2002). Metal carboxylate-phosphonate hybrid layered compounds: Synthesis and single crystal structures of novel divalent metal complexes with N-(phosphonomethyl) iminodiacetic acid, *Inorg. Chem.*, **41**, 2319–2324.

Maroie, S., Savy, M., and Verbist, J. J. (1979). ESCA and EPR studies of monomer, dimer and polymer iron phthalocyanines: Involvements for the electrocatalysis of molecular oxygen reduction, *Inorg. Chem.*, **18**, 2560–2567.

Mateescu, A., Gabriel, C., Raptis, R. G., Baran, P., and Salifoglou, A. (2007). pH-Specific synthesis, spectroscopic, and structural characterization of an assembly of species between Co(II) and N,N-bis(phosphonomethyl)glycine. Gaining insight into metal-ion phosphonate interactions in aqueous Co(II)–organophosphonate systems, *Inorg. Chim. Acta*, **360**, 638–648.

McIntyre, N. S., and Zetaruk, D. G. (1977). X-ray photoelectron spectroscopic studies of iron oxides, *Anal. Chem.*, **49**, 1521–1529.

Meneguzzi, A., Ferreira, C. A., Pham, M. C., Delamar, M., and Lacaze, P. C. (1999). Electrochemical synthesis and characterization of poly(5-amino-1-naphthol) on mild steel electrodes for corrosion protection, *Electrochim. Acta*, **44**, 2149–2156.

Menelaou, M., Dakanali, M., Raptopoulou, C. P., Drouza, C., Lalioti, N., and Salifoglou, A. (2009). pH-Specific synthetic chemistry, and spectroscopic, structural, electrochemical and magnetic susceptibility studies in binary Ni(II)-(carboxy)phosphonate systems, *Polyhedron*, **28**, 3331–3339.

Morad, M. S. (2000). An electrochemical study on the inhibiting action of some organic phosphonium compounds on the corrosion of mild steel in aerated acid solutions, *Corros. Sci.*, **42**, 1307–1326.

Moulder, J. F., Stickle, W. F., Sobol, P. E., and Bamben, K. D. (1995). *Handbook of X-ray Photoelectron Spectroscopy: A Reference Book of Standard Spectra for Identification and Interpretation of XPS Data*, Physical Electronics, Chanhassen, Minn.

Nakayama, N. (2000). Inhibitory effects of nitrilotris(methylenephosphonic acid) on cathodic reactions of steels in saturated $Ca(OH)_2$ solutions, *Corros. Sci.*, **42**, 1897–1920.

Ochoa, N., Baril, G., Moran, F., and Pebere, N. (2002). Study of the properties of a multi-component inhibitor used for water treatment in cooling circuits, *J. Appl. Electrochem.*, **32**, 497–504.

Olivares-Xometl, O., Likhanova, N. V., Martinez-Palou, R., and Dominguez-Aguilar, M. A. (2009). Electrochemistry and XPS study of an imidazoline as corrosion inhibitor of mild steel in an acidic environment, *Mater. Corros.*, **60**, 14–21.

Paszternak, A., Stichleutner, S., Felhosi, I., Keresztes, Z., Nagy, F., Kuzmann, E., Vertes, A., Homonnay, Z., Peto, G., and Kalman, E. (2007). Surface modification of passive iron by alkyl-phosphonic acid layers, *Electrochim. Acta*, **53**, 337–345.

Paszternak, A., Felhosi, I., Paszti, Z., Kuzmann, E., Vertes, A., Kalman, E., and Nyikos, L. (2010). Surface analytical characterization of passive iron surface modified by alkyl-phosphonic acid layers, *Electrochim. Acta*, **55**, 804–812.

Pech-Canul, M. A., and Bartolo-Perez, P. (2004). Inhibition effects of N-phosphono-methyl-glycine/Zn^{2+} mixtures on corrosion of steel in neutral chloride solutions, *Surf. Coat. Technol.*, **184**, 133–140.

Pech-Canul, M. A., and Chi-Canul, L. P. (1999). Investigation of the inhibitive effect of N-phosphono-methyl-glycine on the corrosion of carbon steel in neutral solutions by electrochemical techniques, *Corrosion*, **55**, 948–956.

Pilbath, A., Nyikos, L., Bertoti, I., and Kalman, E. (2008a). Zinc corrosion protection with 1,5-diphosphono-pentane, *Corros. Sci.*, **50**, 3314–3321.

Pilbath, A., Bertoti, I., Sajo, I., Nyikos, L., and Kalman, E. (2008b). Diphosphonate thin films on zinc: Preparation, structure characterization and corrosion protection effects, *Appl. Surf. Sci.*, **255**, 1841–1849.

Pilbath, A., Bertoti, I., Pfeifer, E., Mink, J., Nyikos, L., and Kalman, E. (2009). Formation and characterization of 1,5-diphosphono-pentane films on polycrystalline zinc substrates, *Surf. Coat. Technol.*, **203**, 1182–1192.

Rajendran, S., Appa Rao, B. V., and Palaniswamy, N. (1999a). Synergistic effect of 1-hydroxy-1,1-diphosphonic acid and Zn^{2+} on the inhibition of corrosion of mild steel in neutral aqueous environment, *Anti-corros. Methods Mater.*, **46**, 23–28.

Rajendran, S., Appa Rao, B. V., and Palaniswamy, N. (1999b). Corrosion inhibition by HEDP-Zn^{2+} system for mild steel in low chloride media, *Bull. Electrochem.*, **15**, 131–134.

Rajendran, S., Appa Rao, B. V., and Palaniswamy, N. (2001). Investigation of the inhibiting effect of ethyl phosphonic acid-Zn^{2+} system, *Bull. Electrochem.*, **17**, 171–174.

Reznik, L. Y., Sathler, L., Cardoso, M. J. B., and Albuquerque, M. G. (2008). Experimental and theoretical structural analysis of Zn(II)-1-hydroxyethane-1,1-diphosphonic acid corrosion inhibitor films in chloride ions solution, *Mater. Corros.*, **59**, 685–690.

Sawada, K., Duan, W., Ono, M., and Satoh, K. (2000). Stability and structure of nitrilo(acetate-methylphosphonate) complexes of the alkaline-earth and divalent transition metal ions in aqueous solution, *J. Chem. Soc. Dalton Trans.*, (6), 919–924.

Scheider, W. (1975). Theory of the frequency dispersion of electrode polarization. Topology of networks with fractional power frequency dependence, *J. Phys. Chem.*, **79**, 127–136.

Sekine, I., and Hirakawa, Y. (1986). Effect of 1-hydroxyethylidene-1,1-diphosphonic acid on the corrosion of SS 41 steel in 3% sodium chloride solution, *Corrosion*, **42**, 272–276.

Shaban, A., Kalman, E., and Biczo, I. (1993). Inhibition mechanism of carbon steel in neutral solution by N-phosphono-methyl-glycine, *Corros. Sci.*, **35**, 1463–1470.

Shi Yu, and Gan Moog Chow (2004). Carboxyl group (–CO_2H) functionalized ferromagnetic iron oxide nanoparticles for potential bio-applications, *J. Mater. Chem.*, **14**, 2781–2786.

Telegdi, J., Shaglouf, M. M., Shaban, A., Karman, F. H., Betroti, I., Mohai, M., and Kalman, E. (2001). Influence of cations on the corrosion inhibition efficiency of aminophosphonic acid, *Electrochim. Acta*, **46**, 3791–3799.

To, X. H., Pebere, N., Pelaprat, N., Boutevin, B., and Hervaud, Y. (1997). A corrosion-protective film formed on a carbon steel by an organic phosphonate, *Corros. Sci.*, **39**, 1925–1934.

Touzet, M., Cid, M., Puiggali, M., and Petit, M. C. (1993). An EIS study and auger analysis on 304L stainless steel in hot chloride media before and after a sample straining, *Corros. Sci.*, **34**, 1187–1196.

Wang, C. T., Chen, S. H., Ma, H. Y., and Wang, N. X. (2002). Study of the stability of self-assembled N-vinylcarbazole monolayers to protect copper against corrosion, *J. Serb. Chem. Soc.*, **67**, 685–696.

Westerback, S., Rajan, K. S., and Martell, A. E. (1965). New multidentate ligands. III. Amino acids containing methylenephosphonate groups, *J. Am. Chem. Soc.*, **87**, 2567–2572.

Wu, X., Ma, H., Chen, S., Xu, Z., and Sui, A. (1999). General equivalent circuits for Faradaic electrode processes under electrochemical reaction control, *J. Electrochem. Soc.*, **146**, 1847–1853.